Adsorption of CO_2 and N_2 on Soil Organic Matter: Nature of Porosity, Surface Area, and Diffusion Mechanisms

HUBERT DE JONGE*

Department of Physical Geography and Soil Science, Research Center ARISE, University of Amsterdam, Nieuwe Prinsengracht 130, 1018 VZ Amsterdam, The Netherlands

MARJO C. MITTELMEIJER-HAZELEGER

Department of Chemical Engineering, University of Amsterdam, Amsterdam, The Netherlands

The surface area of soil organic matter (SOM) is a crucial parameter for the interpretation of sorption mechanisms of organic contaminants. The surface area of three SOM samples was studied by using CO_2 and N_2 gas adsorption, revealing that SOM is a microporous material with a high surface area of 94−174 $m^2\ g^{-1}$. The ethylene glycol monoethyl ether (EGME) retention technique has major drawbacks for application to SOM samples, as liquid EGME changes the SOM solid phase density. Nitrogen (N_2) is subject to molecular sieving at 77 K due to activated diffusion in micropores. CO_2 is not limited by activated diffusion since higher experimental temperatures are applied (273 K). About 95−99% of the SOM surface area is formed by micropores with maximum restrictions of approximately 0.5 nm. Results suggest that the diffusion coefficient of CO_2 is influenced by the cross-linking density of the matrix and that the microporous structure is not strongly affected by hydration of the sample. On the basis of pore dimensions, configurational diffusion is proposed as the primary transport mechanism of nonionic organic contaminants in SOM micropores.

Introduction

In spite of the general consensus that soil organic matter (SOM) is the primary adsorbent of hydrophobic organic compounds in wet soils and sediments (*1*, *2*), the sorption mechanism is still a subject of discussion (*3*−*8*). The surface area of SOM is crucial in the mechanistic interpretation of the sorption process. However, large discrepancies were reported (*9*) between SOM surface areas derived from EGME retention (560−800 $m^2\ g^{-1}$) and N_2 adsorption (0.7−18 $m^2\ g^{-1}$). The difference was attributed to an "internal" surface, explored only by the polar adsorbate EGME (*10*). Chiou and coauthors (*11*) argued that EGME causes structural changes to SOM, but this was not irrefutably proved by the data.

N_2 adsorption was recommended (*11*, *47*) as the standard method to measure the surface area of SOM. However, special problems arise for microporous materials when measuring the surface area with N_2 at 77 K. This is well established in allied fields for coal and organic polymers (*12*−*26*). In materials containing pores smaller than 2 nm, the BET−N_2 surface area can be either overestimated as a result of capillary condensation at very low relative pressures (*12*) or underestimated when pores have constrictions smaller than approximately 0.5 nm (*13*, *15*−*17*). As will be explained in the next section, CO_2 is not affected by molecular sieving (*17*−*26*). Therefore, CO_2-derived surface areas of coal and organic polymers were found to be orders of magnitude higher than the N_2 surface areas. Terrestrial and marine humic compounds are considered to be precursors for coal and kerogen materials (*27*). Because they are structurally related, we expected comparable effects with SOM materials. This implies that, until now, the surface area of SOM—as measured with N_2 gas adsorption—might be underestimated by 2 orders of magnitude.

The objective of the present work is to establish the nature of the porosity and surface area of three materials with a high SOM content by comparing adsorption isotherms of N_2 (77 K) with those of CO_2 (273 K). The structure of SOM has been postulated in the literature to be an amorphous cross-linked polymer (*3*), but the low N_2 surface area measurements did not confirm this conceptual model. The CO_2 adsorption data presented here provide evidence for a high surface area, confirming the polymer structure of SOM. In addition, the effect of EGME penetration on the solid phase density of SOM samples is determined. This is a simple but effective way to verify whether the EGME method is suited to measure the surface area of SOM. Finally, results are discussed in relation to the mechanistic interpretation of the diffusion of nonionic organic contaminants in SOM.

Surface Area and Diffusion in Microporous Materials

A theoretical basis for the interpretation of surface area measurements of microporous structures was established in coal and polymer sciences, where the complex nature of these materials was recognized early. When the N_2 surface area of coal was measured, the amount of N_2 adsorbed was found to increase with increasing temperature in the temperature range 77−180 K (*15*). Adsorption is an exothermic process; therefore, the amount adsorbed at equilibrium—at a given relative pressure—must decrease as temperature increases. Hence, it was concluded that sorption equilibrium was not reached at temperatures of 77 K. The kinetics of N_2 adsorption to coal was studied by Zwietering and Van Krevelen (*16*), revealing that the rate of diffusion was positively correlated with temperature. This transport process was called activated diffusion, by analogy with the rate of a chemical reaction.

Activated diffusion was pictured as a process in which a molecule progresses through the polymer network by jumping along a series of adsorption sites. The desorption step from a site requires a finite activation energy, derived

* Corresponding author fax: (+31)20-525-7431.

0013-936X/96/0930-0408$12.00/0

TABLE 1

Particle Size Distribution, Particle External Surface Area, S_{ext}, and Chemical Properties of the Samples

	particle size distribution (μm, mass %)						elemental composition[b] (mass %)					
sample	<20	20−50	50−100	100−500	500−2000	S_{ext}[a] (m^2/g)	C	O	H	N	ash[c]	CEC[a] (mol_c/kg)
humic acid	0.12	0.53	0.95	97.4	0.0	0.0668	38.5	37.3	3.55	0.61	20.0	1.76
Veluwe O_h	0.06	0.23	0.53	34.2	65.0	0.0439	28.5	14.1	4.32	1.37	51.7	1.32
Drenthe peat	0.22	0.61	0.81	35.4	63.0	0.0561	49.5	31.8	4.79	1.28	12.6	0.69

[a] Data expressed on an ash free weight basis. [b] Data expressed on a total dry weight basis. [c] LOI measured for 24 h at 648 K (Veluwe O_h, Drenthe peat) and for 35 h at 773 K (humic acid).

from the temperature dependent vibration amplitudes of the adsorbent and adsorbate. Below a certain temperature, a critical point is reached where molecules are unable to diffuse into the pores. It was shown that N_2 diffusion is restricted when the pore radius is smaller than approximately 0.5 nm by measuring gas adsorption on molecular sieves (*12*). This critical diameter is very close to the molecular diameters of N_2 (0.3 nm) and CO_2 (0.28 nm).

More recently, Rodriguez-Reinoso and co-workers confirmed an increase in the measured N_2 surface area between 77 and 90 K (*18*−*20*). Moreover, if the adsorption at 77 K was carried out under equilibrium conditions—more than 6 weeks to reach equilibrium—the results were coincident with results obtained at 90 K, and with results for the CO_2 surface area measured at 273 K. This clearly confirms that the low surface areas measured with nitrogen are due to the slow diffusion of N_2 into micropores and rules out the possibility that the pore structure itself is affected by low temperatures.

Considering the preceding conclusions, N_2 is not a suitable adsorbate for materials having pores smaller than 0.5 nm, and CO_2 was recognized as a good alternative (*13*, *17*−*26*), primarily because of the higher experimental temperatures that can be applied, usually 273 K. Further, the difference between N_2 and CO_2 adsorption measurements can be used to provide information regarding the pore structure of adsorbents (*17*). The permanent quadrupole moment of CO_2 might cause specific interactions (*14*), but this effect has been shown to be insignificant in the case of active carbons (*25*). Moreover, it is possible to verify whether chemisorption takes place by measuring both adsorption and desorption. Irreversible chemisorption can be ruled out if no hysteresis is observed.

The Dubinin−Radushkevitch (DR) equation is normally used in microporous materials (<2 nm) for the calculation of micropore volume, W_o, and the monolayer equivalent surface area, S_{CO_2}, from the adsorption isotherm in the low relative pressure range (*21*, *28*). Although no theoretical basis exists for the translation of volumetric units to a surface area (*14*), surface areas calculated with the BET and DR models are found to be in excellent concordance in the case where all of the pores have molecular dimensions, such as coal materials (*26*). Therefore, only data up to a relative pressure of 0.02 are needed, and a conventional volumetric apparatus can be used when measuring S_{CO_2}.

Diffusion of organic compounds in zeolite micropores has been studied extensively (*29*). A fundamental difference with diffusion in larger pores is the continuous close contact of the adsorbate with the pore wall. Another important phenomenon besides the above-mentioned activation energy of diffusion is shape selectivity: the diffusion coefficient is strongly affected by molecular size and shape. Relatively small differences in adsorbate diameter or structure can strongly affect diffusion coefficients. Experiments show that the diffusivity of an adsorbate is correlated with the moment of inertia of the adsorbate, suggesting that the diffusion rate is dependent on the rotational freedom of the diffusing molecule (*30*). Therefore, transport in microporous materials is referred to as configurational diffusion. Although the diffusion theory is based on the kinetic theory of gases (*29*, *31*), similar effects have been observed for molecules in the liquid phase (*32*, *33*).

Materials and Methods

Three materials high in organic matter content were used (Table 1). A peat bog was collected from a histosol in Drenthe, The Netherlands. An O_h sample was taken from the most humified horizon of the organic topsoil in a spruce forest at Veluwe, The Netherlands. The samples were air-dried at 323 K for 72 h and passed over a 2 mm sieve without further treatment. A humic acid sample, commercially available (Aldrich H1,675-2) in the sodium salt form, was dissolved in demineralized water (1:50 weight fraction), brought to pH 2.0 with 0.1 M HCl, and allowed to settle for 24 h. Thereafter, the sample was centrifuged for 30 min at 2000 rpm. The precipitate was washed twice with 0.5 and 0.01 M $CaCl_2$, respectively, in order to obtain insoluble humates and then freeze-dried.

Fresh subsamples were used for each measurement. All subsamples were outgassed at 333 K under vacuum ($<10^{-3}$ mbar) for 24 h before N_2 adsorption, CO_2 adsorption, and solid phase density measurements. Thermobalance measurements showed that all physically adsorbed water was removed by this pretreatment.

Nitrogen adsorption measurements were performed in static volumetric equipment (Sorptomatic 1800, Carlo Erba) at 77 K. Sample weight of the O_h and peat samples was about 5 g, and sample weight of the humic acid was about 2 g. The BET theory was used (*14*, *34*) to calculate the surface area S_{N_2} from the linearized BET equation:

$$\frac{p/p_o}{n(1-p/p_o)} = \frac{1}{n_m c} + \frac{c-1}{n_m c}\frac{p}{p_o} \qquad (1)$$

in which p_o is the saturation vapor pressure at the measurement temperature, p/p_o is the relative gas pressure, n is the amount of gas adsorbed per mass of soil, n_m is the monolayer adsorption capacity, and c is a parameter related to the net heat of adsorption. The parameters c and n_m are determined from eq 1, and the surface area S_{N_2} is calculated by multiplying the number of molecules in n_m by the molecular surface area of N_2, A_m (0.162 nm^2).

The same experimental equipment and samples were used for the measurement of CO_2 adsorption isotherms at 273 K. If the rate of pressure decrease was smaller than

TABLE 2

Surface Area (S) and Micropore Volume (W_o) Derived from Gas Adsorption Isotherms[a] and Solid Phase Density, ρ_s, Measured with He, 0.01 M $CaCl_2$, and EGME, Respectively[b]

sample	S_{N_2} (m^2/g)	S_{CO_2} (m^2/g)	W_o (cm^3/g)	$\rho_{s,He}$ (g/cm^3)	$\rho_{s,0.01MCaCl_2}$ (g/cm^3)	$\rho_{s,EGME}$ (g/cm^3)
humic acid	4.94 (3.95)	121 (97)	0.045 (0.036)	1.40 (1.65)	1.58 (1.79)	1.81 (1.98)
Veluwe O_h	0.89 (0.43)	174 (84)	0.064 (0.031)	0.95 (1.83)	1.06 (1.88)	2.44 (2.55)
Drenthe peat	1.10 (0.96)	94 (82)	0.034 (0.030)	1.26 (1.44)	1.21 (1.40)	1.59 (1.72)

[a] Data expressed on an ash free basis; numbers within parentheses are based on total dry weight. [b] SOM density was calculated from bulk solid phase density and ash content, assuming a mineral solid phase density of 2.65 g cm^{-3}. Numbers within parentheses are bulk solid phase densities.

0.132 mbar/15 min, pressure steps were initiated. Pressure in the sample chamber was stored for subsequent data analysis by using a data logger (Campbell Scientific CR10) with sampling intervals of 2 min. The DR equation was used (*14*, *28*) to calculate the microporous volume, W_o, and the monolayer equivalent surface area, S_{CO_2}, according to Dubinin−Kaganer (*14*, *35*) ($A_m = 0.179$ nm^2):

$$\log(W) = \log(W_o) - D \log^2 p/p_o \qquad (2)$$

in which W is the amount adsorbed per mass of soil (expressed as a liquid volume), $W = n/\rho$, in which ρ is the density of the adsorbate in the micropores, W_o is the micropore volume derived from the intercept of the plot of eq 2, and D is a parameter related to the adsorbent−adsorbate pair affinity and the pore size distribution (*14*). The desorption data of CO_2 are limited for practical reasons. The long equilibration time did not allow for measuring the full desorption isotherm, as the temperature could not be maintained at 273 K for longer than 5 days. Therefore, no desorption data for the humic acid sample are available.

A Micromeretics 1305 pycnometer was used for the determination of the solid phase density, $\rho_{s,He}$. The pycnometer method (*36*) was used for measuring the solid phase density in liquid EGME ($\rho_{s,EGME}$) and in a 0.01 M $CaCl_2$ aqueous solution ($\rho_{s,0.01MCaCl_2}$), using separate subsamples for each measurement. Equilibration times were typically 1−2 weeks. Solid phase densities of SOM were derived from the measured density of the bulk material and the ash content, by assuming that the solid phase density of the mineral fraction was 2.65 g cm^{-3}.

In addition to gas adsorption and solid phase densities, characterization of the soils included the following measurements (Table 1): elemental composition (Carlo Erba 1106 elemental analyzer), loss on ignition (*37*), and cation exchange capacity (CEC; *38*, *39*). Furthermore, automated microscopic image analysis (Leica) was performed at magnifications of 25×, 50×, and 100×. The external particle surface area, S_{ext}, was calculated by using the two-dimensional perimeter:area ratio of the particles, thus taking into account the surface roughness at this scale of observation (2−2000 μm). Finally, differential temperature analysis (*40*) was performed by using a platinum−rhodium thermocouple, at a temperature rate of 10 K min^{-1}.

Results

The materials (Table 1) were especially suited to measure the surface area of SOM (Table 2) because either the mineral fraction was very low, which was the case for the humic acid and the peat sample, or the mineral fraction consisted of coarse silica with negligible surface area (Veluwe O_h). The two natural soils have a comparable elemental composition, while the humic acid differs considerably from the two other soils: the O:C ratio of the humic acid is much higher than those of the other samples, which is probably caused by a higher functional group density (Table 1). Furthermore, differential temperature analysis revealed that the O_h and peat samples have exothermic peaks at 510 and 673 K (50%, 50%), whereas humic acid shows a main exothermic reaction at 800 K (80%) and a minor one at 500 K (20%).

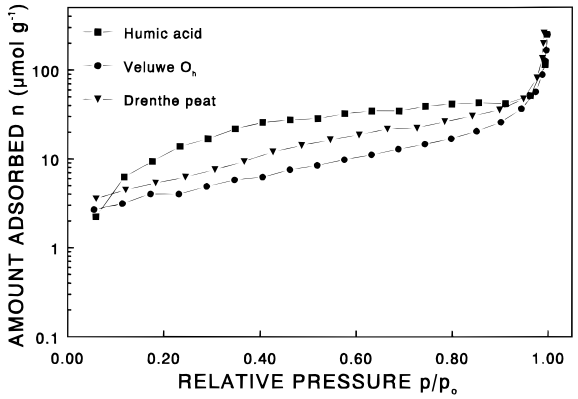

FIGURE 1. N_2 gas adsorption isotherms of the three samples. The experimental temperature was 77 K. Note that the ordinate is in logarithmic units.

In Figure 1, N_2 adsorption isotherms are presented with a logarithmic ordinate, which is quite unusual, and show that n is very small over a large relative pressure range. As a result, the measurement itself is not very accurate; however, the values of the BET surface areas that were derived (Table 2) are in agreement with values for SOM samples reported earlier (*9*).

Adsorption isotherms of CO_2 and DR plots of the three materials are shown in Figure 2. The limited available desorption data are also given in Figure 2A, showing no hysteresis of the isotherm. Compared to the N_2 isotherms, the relative pressure range of the CO_2 isotherms is smaller, while the amount adsorbed at a certain value of p/p_o is much higher. The shapes of the isotherms of the peat and the O_h samples are identical. Further, the DR plots are almost linear, indicating that the two samples have a narrow pore size distribution. By contrast, the isotherm of the humic acid is almost linear, and the slope of the DR plot considerably deviates from those of the other two samples. The monolayer equivalent surface areas of the three materials are presented in Table 2 and Figure 3, showing that S_{CO_2} is approximately 25−200 times higher than S_{N_2}, while S_{N_2} is 1−2 orders of magnitude higher than S_{ext}, the particle surface area determined with quantitative microscopic analysis. Values of S_{CO_2} are on the same order of magnitude as coal materials, having surface areas of approximately 200 m^2 g^{-1} (*21*).

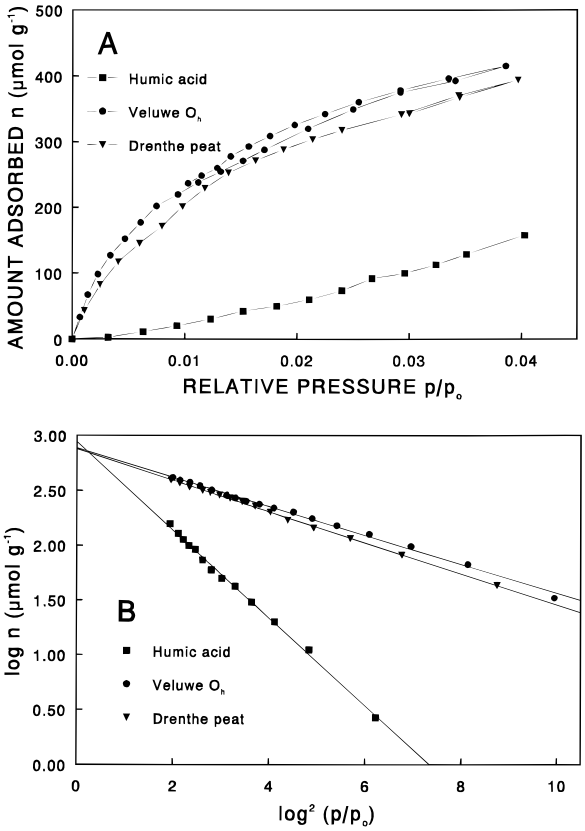

FIGURE 2. CO_2 gas adsorption isotherms (A) and the Dubinin–Radushkevich plots (B) of the three samples. The desorption isotherm was partly measured for the Veluwe O_h and peat samples; these data are also shown in part A. The experimental temperature was 273 K.

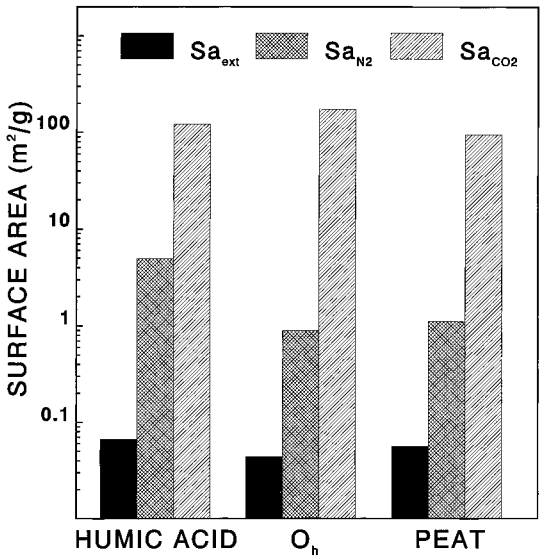

FIGURE 3. Surface area of the three samples measured with quantitative microscopic analysis (S_{ext}) and gas adsorption isotherms (S_{N_2}, S_{CO_2}). Surface areas are based on an ash free weight basis.

Figure 4 shows the CO_2 pressure dynamics in the sample chamber during the first five gas volume additions. The decrease with time—after the addition of a volume of gas to the sample chamber—reflects the CO_2 adsorption kinetics. The equilibration time of CO_2 adsorption on the O_h and peat samples was about 5–10 h, while N_2 adsorption reached an apparent equilibrium in 10–20 min (data not shown). The writing recorder showed a very fast (<2 min)

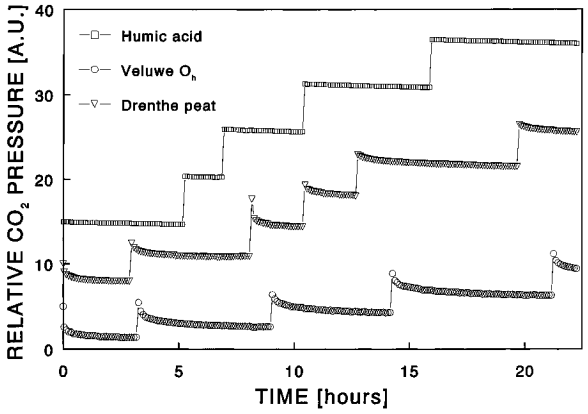

FIGURE 4. Pressure dynamics of CO_2 in the sample chamber, reflecting the adsorption kinetics of CO_2 during the first five gas volume additions. The ordinate has an arbitrary pressure dimension, and signals have a different offset at time $t = 0$ to allow visual comparison.

initial CO_2 adsorption phase for the humic acid that was not recorded on the data logger as the sampling rate was too large (2 min). This almost instantaneous adsorption phase therefore is not shown in Figure 4. The actual amount of CO_2 adsorbed, however, is comparable to that in the other two samples. Obviously, the surface explored by CO_2 molecules is highly influenced by the delay between consecutive volume additions; if this period is too short, n will be underestimated. This was the case for the humic acid sample, showing a very slow decrease in pressure without equilibrium being reached between consecutive volume additions (Figure 4). Therefore, the surface area of this sample probably was not correctly determined.

Liquid EGME strongly increases the solid phase density of the materials compared to $\rho_{s,He}$ (Table 2). Volumetric EGME capacity was 0.134, 0.204, and 0.146 $cm^3\,g^{-1}$ for humic acid, O_h, and peat, respectively. The densities in an aqueous solution (0.01 M $CaCl_2$) are identical, within measurement accuracy, to $\rho_{s,He}$, except for the humic acid sample.

Discussion

The main result of this study is the large difference found between the BET–N_2 surface area (0.89–4.94 $m^2\,g^{-1}$) and the much higher CO_2 surface area (94–174 $m^2\,g^{-1}$). The question is not whether either of these two methods is "superior"; the crucial issue of this article is that a comparison of the results from these two techniques allows for the important conclusion that SOM has a polymer structure with a very high surface area formed by pores with restrictions of approximately 0.5 nm.

This conclusion can be drawn by analogy with surface area measurements of coal materials and other polymers (*15–26*). The micropores can, under measuring conditions, be penetrated only by CO_2 and not by N_2 due to activated diffusion. Nitrogen molecules are subject to molecular sieving at the experimental temperature of 77 K; hence, only a small fraction (1–5%) of the total surface area is explored. The measured S_{N_2} is about 10–100 times higher than the external particle surface area that was estimated from microscopic analysis (about 0.05 $m^2\,g^{-1}$, Table 1). This difference could be attributed to an "external" surface formed by pores that are accessible to N_2 at 77 K. However, the physical interpretation of S_{N_2} as an external surface area is doubtful, since it is very well possible that the surface area is overestimated due to capillary condensation of N_2 in pores of 0.5–2.0 nm (*12*).

By definition, an adsorbate used for surface area measurements should not change the structure of the adsorbent. Therefore, it must be concluded that in a strict sense the EGME method is not suited for SOM, as the measured solid phase densities of the samples are significantly changed when saturated with EGME (Table 2). It is most unlikely that EGME can penetrate directly into micropores that are inaccessible to helium, as helium is by far the smallest molecule. Hence, the increased density must be attributed to the alteration of the micropore structure of SOM by EGME, probably due to favorable physical interactions. As a consequence, EGME-derived monolayer equivalent surface areas reported earlier are unrealistically high.

The reversibility of the sorption of CO_2 to SOM samples (Figure 2A) indicates that CO_2 is not affected by chemisorption. Therefore, sorption kinetics can be related to mass transport into the SOM micropores. Given the large difference between S_{N_2} and S_{CO_2}, the majority of internal pores must have limiting restrictions that are approximately 0.5 nm. The micropores in the samples have a narrow size distribution, as indicated by the linearity of the DR plots (Figure 2B), but no direct information can be obtained about pore shape. However, adsorption kinetics might contain information about the pore structure. The approach to equilibrium of the humic acid sample is much slower than those of to the other two samples (Figure 4). Humic acid also has the highest solid phase density (Table 2) and much higher temperatures of exothermic reaction. The structure of the humic acid sample is built up with more soluble, smaller molecules, giving rise to a higher degree of cross-linking. This in turn will lead to a higher chance of entanglement of the adsorbate with the matrix. All of these aspects result in a lower expected diffusion constant, which is clearly confirmed by our measurements. In brief, our data suggest that CO_2 diffusion rates are related to the structural properties of the micropores.

Care must be taken in the interpretation of the CO_2-derived surface area for several reasons. First, true equilibrium must be reached, and this possibly was not the case with the humic acid sample within 10 h. Second, and more importantly, it is debatable whether to use the surface area concept for a polymer structure in which pores have the same scale as the penetrating molecules, since there is no clear pore−surface interface as there is in larger pores. An alternative would be to use volume or capacity units, which is the normal fashion with microporous materials (*14*). The third reason is that the structure of SOM is not rigid. It can be argued that the structure of SOM is affected by hydration, and therefore the structure was changed during outgassing of the sample prior to gas adsorption measurements. However, we expect that this will mainly influence macropores in the material and that the micropore volume will remain unaffected when the material is hydrated. This is confirmed by observing the densities in an aqueous solution (0.01 M $CaCl_2$) of the two natural organic soils. They were not significantly different from the densities measured with helium. The humic acid sample, however, shows a significant increase in density, reflecting a larger water soluble fraction. Therefore, structural change after drying of a sample is dependent on the composition of SOM, and changes are expected to be stronger when the sample contains more water soluble components.

The results described provide important implications for the interpretation of sorption mechanisms of organic contaminants in SOM. Only nonionic organic contaminants will be discussed; therefore, chemical interactions can be excluded. Our data support the concept of intraorganic matter diffusion as "mesh" diffusion in an amorphous, cross-linked polymer (*3*, *41*). Moreover, quantitative estimates of pore size and surface area derived from CO_2 adsorption allow for a more specific formulation of this concept. The majority of total surface area is formed by subnanometer scale pores. Hence, sorption kinetics will be significantly influenced by transport in these pores.

We expect that the diffusion of gas and liquid molecules in SOM micropores can be described by using the concept of configurational diffusion (see the theory section). By applying this concept to SOM, very low diffusion coefficients are generally expected. Furthermore, it is expected that diffusion rates will be strongly temperature dependent and that diffusion rates will also be strongly dependent on molecular size and shape. For example, consider that benzene, a planar molecule, has three principal molecular diameters of 0.66, 0.73, and 0.35 nm (*14*). It is clear that even this relatively simple molecule will experience spheric hindrance in the SOM matrix. It will only be able to enter slit-shaped pores, since our data indicate that restrictions are about 0.4−0.5 nm.

It is also important to recognize that SOM has a highly heterogeneous chemical structure (*42*), as it consists of humic substances, carbohydrates, and lignin-related compounds. Therefore, the surface is heterogeneous over molecular scale distances, giving rise to distinct gradients in the chemical potential in micropores. Considering this, it is expected (*3*) that within micropores sites exist—cages or dead-end pores—in which molecules become effectively trapped. Given a certain pore structure, the probability of immobilization of an adsorbate is expected to increase with the moment of inertia of the adsorbate (*30*). An exception to this rule is that compounds that can form hydrogen bonds, for example, phenolic compounds, are expected to be more strongly adsorbed to the matrix. This is due to the higher activation energy of a hydrogen bond than nonspecific van der Waals interactions. A final consideration is that the diffusivity of an adsorbate will also be affected by the hydration of the SOM matrix. If micropores are hydrated, counterdiffusion of water molecules must take place during the uptake of an adsorbate. This will significantly influence the effective diffusion coefficient.

The above-described concept is in agreement with literature concerning the sorption of nonionic organic compounds on SOM. There is increasing evidence for a "resistant" fraction associated with very low mass transfer rates. This fraction increases with contact time with the soil or sediment, as was shown, for example, for various haloaliphatic compounds and naphthalene (*3*, *43*, *44*). Extremely long equilibration times—up to decades—were reported for desorption of the fumigant 1,2-dibromoethane (EDB), despite the fact EDB is a compound with a relatively low log K_{ow} (1.5−2.1), and no chemical interactions are expected (*45*). Desorption rates were found to be strongly affected by temperature. From the perspective of configurational diffusion, compounds containing Br are expected to be easily immobilized due to its large van der Waals radius: 0.39 nm. Finally, direct studies of Brusseau and coauthors (*41*, *46*) have shown that adsorbate structure strongly influences diffusion rates.

Acknowledgments

The authors are grateful to J. I. Freijer, H. A. J. Govers, L. W. Petersen, J. M. Verstraten, and D. Warmerdam for their comments and suggestions.

Literature Cited

(1) Chiou, C. T. In *Reactions and Movement of Organic Chemicals in Soils*; Linn, D. M., Ed.; SSSA Spec. Publ. 22, SSSA and ASA: Madison, WI, 1989; p 1.
(2) Scow, K. M. In *Sorption and Degradation of Pesticides and Organic Chemicals in Soils*; Linn, D. M., Ed.; SSSA Spec. Publ. 32, SSSA and ASA: Madison, WI, 1993; p 73.
(3) Pignatello, J. J. In *Reactions and Movement of Organic Chemicals in Soils*; SSSA Spec. Publ. 22, SSSA and ASA: Madison, WI, 1989; p 45.
(4) Chiou, C. T.; Peters, L. J., Freed, V. H. *Science* **1979**, *206*, 831.
(5) Chiou, C. T.; Porter, P. E.; Schmedding, D. W. *Environ. Sci. Technol.* **1983**, *17*, 227.
(6) Chiou, C. T.; Rutherford, D. W. *Environ. Sci. Technol.* **1993**, *27*, 1587.
(7) Weber, W. J., Jr.; McGinley, P. M.; Katz, L. E. *Environ. Sci. Technol.* **1992**, *26*, 1955.
(8) McGinley, P. M.; Katz, L. E.; Weber, W. J., Jr. *Environ. Sci. Technol.* **1993**, *27*, 1524.
(9) Chiou, C. T.; Lee, J.-F.; Boyd, S. A. *Environ. Sci. Technol.* **1990**, *24*, 1164.
(10) Pennell, K. D.; Rao, P. S. C. *Environ. Sci. Technol.* **1992**, *26*, 402.
(11) Chiou, C. T.; Lee, J.-F.; Boyd, S. A. *Environ. Sci. Technol.* **1992**, *26*, 404.
(12) Lamond, T. G.; Marsh, H. *Carbon* **1964a**, *1*, 281.
(13) Marsh, H.; Wynne-Jones, W. F. K. *Carbon* **1964**, *1*, 269.
(14) Greg, S. J.; Sing, K. S. W. *Adsorption, Surface Area and Porosity*, 2nd ed.; Academic Press: London, 1982.
(15) Maggs, F. A. P. *Research* **1953**, *6*, 513.
(16) Zwietering, P.; van Krevelen, D. W. *Fuel* **1954**, *33*, 331.
(17) Garrido, J.; Linares-Solano, A.; Martin-Martinez, J. M.; Molina-Sabio, M.; Rodriguez-Reinoso, F.; Torregrosa, R. *Langmuir* **1987**, *3*, 76.
(18) Rodriguez-Reinoso, F.; Lopez-Gonzalez, J. D.; Berenguer, C. *Carbon* **1982**, *20*, 513.
(19) Rodriguez-Reinoso, F.; Lopez-Gonzalez, J. D.; Berenguer, C. *Carbon* **1982**, *22*, 13.
(20) Rodriguez-Reinoso, F. In *Carbon and Coal Gasification, Science and Technology*; Figueiredo, J. L., Moulijn, J. A., Eds.; Martinus Nijhoff: Dordrecht, The Netherlands, 1986; pp 601−642.
(21) Marsh, H.; Siemieniewska, T. *Fuel* **1965**, *44*, 355.
(22) Lamond, T. G.; Metcalfe, J. E.; Walker, P. L., Jr. *Carbon* **1965**, *3*, 59.
(23) Kipling, J. J.; Sherwood, J. N.; Shooter, P. V.; Thomson, H. R.; Young, R. N. *Carbon* **1966**, *4*, 5.
(24) Debalak, K. A.; Schrodt, J. T. *Fuel* **1979**, *58*, 723.
(25) Lamond, T. G.; Marsh, H. *Carbon* **1964b**, *1*, 293.
(26) Walker, P. L., Jr.; Patel, R. L. *Fuel* **1970**, *49*, 91.
(27) Grathwohl, P. *Environ. Sci. Technol.* **1990**, *24*, 1687.
(28) Dubinin, M. M.; Radushkevich, L. V. *Proc. Acad. Sci. USSR* **1947**, *55*, 331.
(29) Wei, J. *Ind. Eng. Chem. Res.* **1994**, *33*, 2467.
(30) Rutven, D. M.; Kaul, B. K. *Ind. Eng. Chem. Res.* **1993**, *32*, 2035.
(31) Krishna R. *Gas Sep. Purif.* **1993**, *7*, 91.
(32) Moore, R. M.; Katzer, J. R. *AIChE J.* **1972**, *18*, 816.
(33) Satterfield, C. N.; Colton, C. K.; Pitcher, W. H., Jr. *AIChE J.* **1973**, *19*, 628.
(34) Brunnauer, S.; Emmet, P. H.; Teller, E. *J. Am. Chem. Soc.* **1938**, *60*, 309.
(35) Kaganer, M. G. *Zh. Fiz. Khim.* **1959**, *33*, 2202.
(36) Blake, G. R.; Hartge, K. H. In *Methods of Soil Analysis. Part I. Physical and Mineralogical Methods*; Klute, A., Ed.; Am. Soc. Agronomy: Madison, WI, 1986; Chapter 14.
(37) Chin Huat Lim; Jackson, M. L. In *Methods of Soil Analysis. Part I. Physical and Mineralogical Methods*; Klute, A., Ed.; Am. Soc. Agronomy: Madison, WI, 1986; Chapter 1.
(38) Gillman, G. P. *Austr. J. Soil Res.* **1979**, *17*, 129.
(39) Rhoades, J. D. In *Methods of Soil Analysis. Part II. Chemical and Microbiological Properties*; Page, A. L., Miller, R. H., Keeney, D. R., Eds.; Am. Soc. Agronomy: Madison, WI, 1982; Chapter 8.
(40) Tan, K. H.; Hajek, B. F.; Barshad, I. In *Methods of Soil Analysis. Part I. Physical and Mineralogical Methods*; Klute, A., Ed.; Am. Soc. Agronomy: Madison, WI, 1986; Chapter 7.
(41) Brusseau, M. L.; Jessup, R. E.; Rao, P. S. C. *Environ. Sci. Technol.* **1991**, *25*, 134.
(42) Ziechmann, W. In *Humic Substances and Their Role in the Environment*; Frimmel, F. H., Christman, R. F., Eds.; Wiley: New York, 1988; p 113.
(43) Brusseau, M. L.; Rao, P. S. C. *Crit. Rev. Environ. Control* **1989**, *19*, 33.
(44) Connaughton, D. F.; Stedinger, J. R.; Lion, L. W.; Shuler, M. L. *Environ. Sci. Technol.* **1993**, *27*, 2397.
(45) Steinberg, S. M.; Pignatello, J. J.; Sawhney, B. L. *Environ. Sci. Technol.* **1987**, *21*, 1201.
(46) Brusseau, M. L.; Rao, P. S. C. *Environ. Sci. Technol.* **1991**, *25*, 1501.
(47) Pennel, K. D.; Boyd, S. A.; Abriola, L. M. *Soil Sci. Soc. Am. J.* **1995**, *59*, 1012.

Received for review January 25, 1995. Revised manuscript received August 14, 1995. Accepted September 8, 1995.[⊗]

ES950043T

[⊗] Abstract published in *Advance ACS Abstracts,* December 1, 1995.